

# Discovery of the spectroscopic binary nature of six southern Cepheids

L. Szabados,<sup>1</sup>\* A. Derekas,<sup>1,2</sup> L. L. Kiss,<sup>1,2,3</sup> J. Kovács,<sup>3</sup> R. I. Anderson,<sup>4</sup> Cs. Kiss,<sup>1</sup>  
T. Szalai,<sup>5</sup> P. Székely<sup>6</sup> and J. L. Christiansen<sup>7</sup>

<sup>1</sup>Konkoly Observatory, Research Centre for Astronomy and Earth Sciences, Hungarian Academy of Sciences, Konkoly Thege Miklós út 15-17, H-1121 Budapest, Hungary

<sup>2</sup>Sydney Institute for Astronomy, School of Physics, University of Sydney, NSW 2006, Australia

<sup>3</sup>ELTE Gothard-Lendület Research Group, Szent Imre herceg út 112, H-9700 Szombathely, Hungary

<sup>4</sup>Observatoire de Genève, Université de Genève, 51 Ch. des Maillettes, CH-1290 Versoix, Switzerland

<sup>5</sup>Department of Optics and Quantum Electronics, University of Szeged, Dóm tér 9, H-6720 Szeged, Hungary

<sup>6</sup>Department of Experimental Physics, University of Szeged, H-6720 Szeged, Hungary

<sup>7</sup>SETI Institute/NASA Ames Research Center, M/S 244-30, Moffett Field, CA 94035, USA

Accepted 2013 January 3. Received 2013 January 3; in original form 2012 November 22

## ABSTRACT

We present the analysis of photometric and spectroscopic data of six bright Galactic Cepheids: GH Carinae, V419 Centauri, V898 Centauri, AD Puppis, AY Sagittarii and ST Velorum. Based on new radial velocity data (in some cases supplemented with earlier data available in the literature), these Cepheids have been found to be members in spectroscopic binary systems. V898 Cen turned out to have one of the largest orbital radial velocity amplitude ( $>40 \text{ km s}^{-1}$ ) among the known binary Cepheids. The data are insufficient to determine the orbital periods nor other orbital elements for these new spectroscopic binaries.

These discoveries corroborate the statement on the high frequency of occurrence of binaries among the classical Cepheids, a fact to be taken into account when calibrating the period–luminosity relationship for Cepheids.

We have also compiled all available photometric data that revealed that the pulsation period of AD Pup, the longest period Cepheid in this sample, is continuously increasing with  $\Delta P = 0.004567 \text{ d century}^{-1}$ , likely to be caused by stellar evolution. The wave-like pattern superimposed on the parabolic  $O - C$  graph of AD Pup may well be caused by the light-time effect in the binary system. ST Vel also pulsates with a continuously increasing period. The other four Cepheids are characterized with stable pulsation periods in the last half century.

**Key words:** binaries: spectroscopic – stars: variables: Cepheids.

## 1 INTRODUCTION

Classical Cepheid variable stars are primary distance indicators because owing to the famous period–luminosity ( $P-L$ ) relationship they rank among standard candles in establishing the cosmic distance scale.

Companions to Cepheids, however, complicate the situation. The contribution of the secondary star to the observed brightness has to be taken into account when involving any particular Cepheid in the calibration of the  $P-L$  relationship. Binaries among Cepheids are not rare at all: their frequency exceeds 50 per cent for the brightest Cepheids, while among the fainter Cepheids an observational selection effect encumbers revealing binarity (Szabados 2003a).

It is essential to study Cepheids individually from the point of view of binarity before involving them in any calibration procedure

(of e.g.  $P-L$  or period–radius relationship). This attitude is especially important if Cepheid-related relationships are calibrated using a small sample. However, a deep observational analysis of individual Cepheids can only be performed in the case of their Galactic representatives. When dealing with extragalactic Cepheids, unrevealed binarity is one of the factors that contributes to the dispersion of the  $P-L$  relationship. A detailed list of physical factors responsible for the finite width of the  $P-L$  relationship around the ridge line approximation is given by Szabados & Klagyivik (2012).

The orbital period of binaries involving a supergiant Cepheid component cannot be shorter than about a year. Spectroscopic binaries involving a Cepheid component with orbital periods longer than a decade are also known (see the online data base on binaries among Galactic Cepheids: <http://www.konkoly.hu/CEP/orbit.html>). Therefore, a first epoch radial velocity (RV) curve, especially based on data obtained in a single observational season, is usually insufficient for pointing out an orbital effect superimposed on the RV changes due to pulsation.

\* E-mail: szabados@konkoly.hu

**Table 1.** Basic data of the programme stars and the number of spectra.

Star	$V$ (m)	$P$ (d)	Mode of pulsation	No. of obs.
GH Car	9.18	5.725 532	First overtone	27+43
V419 Cen	8.19	5.507 123	First overtone	26
V898 Cen	8.00	3.527 310	First overtone	33+4
AD Pup	9.91	13.596 919	Fundamental	33
AY Sgr	10.55	6.569 667	Fundamental	22
ST Vel	9.73	5.858 316	Fundamental	27

In the case of pulsating variables, like Cepheids, spectroscopic binarity (SB) manifests itself in a periodic variation of the  $\gamma$ -velocity (i.e. the RV of the mass centre of the Cepheid). In practice, the orbital RV variation of the Cepheid component is superimposed on the RV variations of pulsational origin. To separate the orbital and pulsational effects, knowledge of the accurate pulsation period is essential, especially when comparing RV data obtained at widely differing epochs. Therefore, the pulsation period and its variations have been determined with the method of the  $O - C$  diagram (Sterken 2005) for each target Cepheid. Use of the accurate pulsation period obtained from the photometric data is a guarantee for the correct phase matching of the (usually less precise) RV data.

In this paper, we point out SB of six bright Galactic Cepheids by analysing RV data. The structure of this paper is as follows. The new observations and the equipments utilized are described in Section 2. Section 3 is devoted to the results on the six new SB Cepheids: GH Carinae, V419 Centauri, V898 Centauri, AD Puppis, AY Sagittarii and ST Velorum, respectively. Basic information on these Cepheids is found in Table 1. Finally, Section 4 contains our conclusions.

## 2 NEW OBSERVATIONS

### 2.1 Spectra from Siding Spring Observatory

We performed a RV survey of Cepheids with the 2.3 m ANU telescope located at Siding Spring Observatory (SSO), Australia. The main aim of the project was to detect Cepheids in binary systems by measuring changes in the mean values of their RV curve which can be interpreted as the orbital motion of the Cepheid around the centre of mass in a binary system (change of  $\gamma$ -velocity). The target list was compiled to include Cepheids with single epoch RV phase curve or without any published RV data. Several Cepheids suspected members in spectroscopic binaries were also put on the target list. On 64 nights between 2004 October and 2006 March we monitored 40 Cepheids with pulsation periods between 2 and 30 d. (V898 Cen was observed in 2009 July too).

Medium-resolution spectra were taken with the Double Beam Spectrograph using the 1200 mm<sup>-1</sup> gratings in both arms of the spectrograph. The projected slit width was 2 arcsec on the sky, which was about the median seeing during our observations. The spectra covered the wavelength ranges 4200–5200 Å in the blue arm and 5700–6700 Å in the red arm. The dispersion was 0.55 Åpx<sup>-1</sup>, leading to a nominal resolution of about 1 Å.

All spectra were reduced with standard tasks in IRAF.<sup>1</sup> Reduction consisted of bias and flat-field corrections, aperture extraction,

wavelength calibration and continuum normalization. We checked the consistency of wavelength calibrations via the constant positions of strong telluric features, which proved the stability of the system. RVs were determined only for the red arm data with the task *fxcor*, applying the cross-correlation method using a well-matching theoretical template spectrum from the extensive spectral library of Munari et al. (2005). Then, we made barycentric corrections to every single RV value. This method resulted in a 1–2 km s<sup>-1</sup> uncertainty in the individual RVs, while further tests have shown that our absolute velocity frame was stable to within  $\pm 2$ –3 km s<sup>-1</sup>. This level of precision is sufficient to detect a number of Cepheid companions, as they can often cause  $\gamma$ -velocity changes well above 10 km s<sup>-1</sup>.

### 2.2 FEROS observations in ESO

V898 Centauri was observed on four consecutive nights in 2011 April, using the Fiber-fed Extended Range Optical Spectrograph (FEROS) instrument on the MPG/European Southern Observatory (ESO) 2.2 m telescope in La Silla Observatory, Chile (see Table 10). The FEROS has a total wavelength coverage of 356–920 nm with a resolving power of  $R = 48\,000$  (Kaufer et al. 1999, 2000). Two fibres, with entrance aperture of 2.7 arcsec, simultaneously recorded star light and sky background. The detector is a back-illuminated CCD with 2948 × 4096 pixels of 15 μm size. Basic data reduction was performed using a pipeline package for reductions (DRS), in MIDAS environment. The pipeline performs the subtraction of bias and scattered light in the CCD, orders extraction, flat-fielding and wavelength calibration with a ThAr calibration frame (the calibration measurements were performed at the beginning of each night, using the ThAr lamp).

After the continuum normalization of the spectra using IRAF we determined the RVs with the task *fxcor*, as in the case of the SSO spectra (see Section 2.1). The velocities were determined in the region 500–600 nm, where a number of metallic lines are present and hydrogen lines are lacking. We made barycentric corrections to each RV value with the task *rvcorrect*. The estimated uncertainty of the RVs is 0.05 km s<sup>-1</sup>.

### 2.3 CORALIE observations from La Silla

GH Car was among the targets during multiple observing campaigns between 2011 April and 2012 May using the fibre-fed high-resolution ( $R \sim 60\,000$ ) echelle spectrograph CORALIE mounted at the Swiss 1.2 m Euler telescope at ESO La Silla Observatory, Chile. The instrument's design is described in Queloz et al. (2001); recent instrumental updates are found in Wilson et al. (2008).

The spectra are reduced by the efficient online reduction pipeline that performs bias correction, cosmic removal and flat-fielding using tungsten lamps. ThAr lamps are used for the wavelength calibration. The reduction pipeline directly determines the RV through cross-correlation (Baranne et al. 1996) using a mask that resembles a G2 spectral type. The RV stability of the instrument is excellent and for non-pulsating stars the RV precision is limited by photon noise, see e.g. Pepe et al. (2002). However, the precision achieved for Cepheids is lower due to line asymmetries. We estimate a typical precision of  $\sim 0.1$  km s<sup>-1</sup> (including systematics due to pulsation) per data point for our data. The RV data are listed in Table 4.

<sup>1</sup> IRAF is distributed by the National Optical Astronomy Observatories, which are operated by the Association of Universities for Research in Astronomy, Inc., under cooperative agreement with the National Science Foundation.

### 3 RESULTS

#### 3.1 GH Carinae

*Accurate value of the pulsation period.* The brightness variability of GH Car (HD 306077,  $\langle V \rangle = 9.18$  mag) was revealed by Oosterhoff (Hertzsprung 1930). This Cepheid pulsates in the first overtone mode, therefore, it has a small pulsational amplitude and nearly sinusoidal light (and velocity) curve.

In the case of Cepheids pulsating with a low amplitude, the  $O - C$  diagram constructed for the median brightness is more reliable than that based on the moments of photometric maxima (Derekas et al. 2012). Therefore, we determined the accurate value of the pulsation period by constructing an  $O - C$  diagram for the moments of median brightness (the mid-point between the faintest and the brightest states) on the ascending branch of light curve since it is this phase when the brightness variations are steepest during the whole pulsational cycle.

All published observations of GH Car covering half a century were re-analysed in a homogeneous manner to determine seasonal moments of the chosen light curve feature. The relevant data listed in Table 2 are as follows.

Col. 1: Heliocentric moment of the median brightness on the ascending branch;

Col. 2: epoch number,  $E$ , as calculated from equation (1):

$$C = 2451\,266.2198 + 5.725\,532 \times E \pm 0.0038 \pm 0.000\,004 \quad (1)$$

**Table 2.**  $O - C$  values of GH Carinae (see the description in Section 3.1).

JD <sub>⊙</sub> 240 0000+	$E$	$O - C$	$W$	Data source
351 48.8988	-2815	+0.0516	2	Walraven, Muller & Oosterhoff (1958)
352 28.9336	-2801	-0.0711	2	Irwin (1961)
407 59.8900	-1835	+0.0214	3	Pel (1976)
441 32.1611	-1246	-0.0458	3	Berdnikov (2008)
481 68.7453	-541	+0.0383	2	<i>Hipparcos</i> (ESA 1997)
486 61.1326	-455	+0.0299	2	<i>Hipparcos</i> (ESA 1997)
495 42.9049	-301	+0.0702	2	Berdnikov (2008)
498 17.6922	-253	+0.0320	3	Berdnikov (2008)
503 90.1805	-153	-0.0329	3	Berdnikov (2008)
505 73.3930	-121	-0.0374	3	Berdnikov (2008)
508 94.0822	-65	+0.0220	3	Berdnikov (2008)
512 66.2270	0	+0.0072	3	Berdnikov (2008)
516 55.5715	68	+0.0155	3	Berdnikov (2008)
519 53.2783	120	-0.0053	2	ASAS (Pojmanski 2002)
519 58.9981	121	-0.0111	3	Berdnikov (2008)
523 48.3311	189	-0.0142	2	ASAS (Pojmanski 2002)
523 59.7765	191	-0.0199	3	Berdnikov (2008)
526 51.8321	242	+0.0336	3	Berdnikov (2008)
527 83.4687	265	-0.0171	3	ASAS (Pojmanski 2002)
529 72.4125	298	-0.0158	1	<i>INTEGRAL</i> OMC
530 12.4642	305	-0.0429	3	Berdnikov (2008)
531 09.8033	322	-0.0378	2	ASAS (Pojmanski 2002)
534 64.8631	384	+0.0390	3	ASAS (Pojmanski 2002)
537 96.9347	442	+0.0298	3	ASAS (Pojmanski 2002)
542 26.3353	517	+0.0155	3	ASAS (Pojmanski 2002)
545 18.3336	568	+0.0116	3	ASAS (Pojmanski 2002)
546 21.3538	586	-0.0278	3	ASAS (Pojmanski 2002)
548 50.4167	626	+0.0139	3	ASAS (Pojmanski 2002)
549 70.5964	647	-0.0426	3	ASAS (Pojmanski 2002)

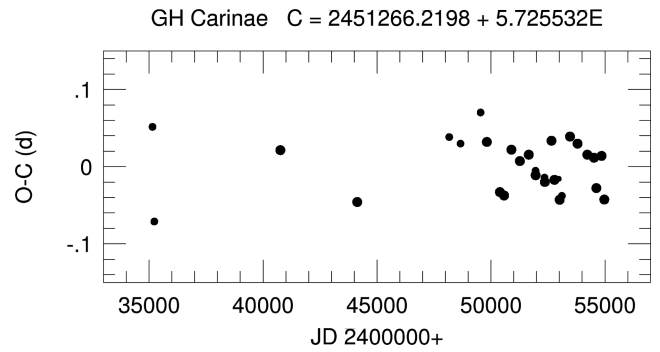


**Figure 1.**  $O - C$  diagram of GH Car based on the values listed in Table 2. The pulsation period of GH Car is constant.

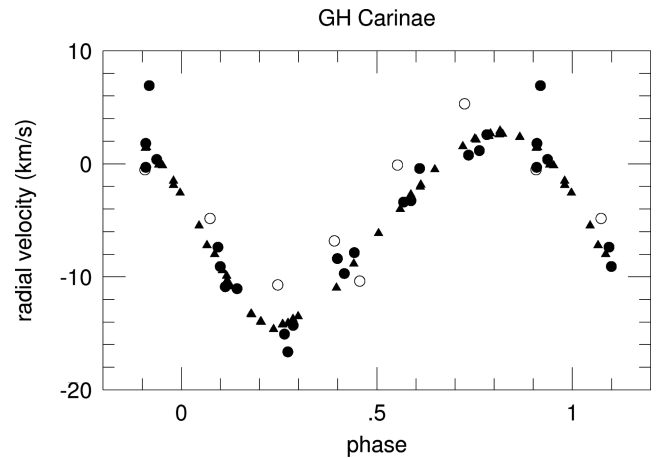


**Figure 2.** RV phase curve of GH Carinae. The filled circles represent data from 2004–2005, the open circles denote data from 2006, while the CORALIE data obtained in 2011–2012 are marked as triangles.

(this ephemeris has been obtained by the weighted least-squares fit to the tabulated  $O - C$  differences);

Col. 3: the corresponding  $O - C$  value as calculated from equation (1);

Col. 4: weight assigned to the  $O - C$  value (1, 2 or 3 depending on the quality of the light curve leading to the given difference);

Col. 5: reference to the origin of data, preceded by the name of the observer if different from the author(s) cited.

The plot of  $O - C$  values shown in Fig. 1 can be approximated with a constant period. The scatter of the points in the figure reflects the observational error and uncertainties in the analysis of the data.

*Binarity of GH Car.* There are no published RV data for this bright Cepheid. The phase diagram of our RV observations is plotted in Fig. 2. The observational data have been folded on the period given by the ephemeris in equation (1). The zero phase has been arbitrarily chosen at JD 240 0000 (similarly to all phase curves in this paper). Fig. 2 clearly shows a vertical shift between the mean values valid for 2004–2005 and 2006. For the first season, the  $\gamma$ -velocity (the mean RV averaged over a pulsational cycle) was  $-4.6$  km s $^{-1}$ , while one year later it became  $-3.5$  km s $^{-1}$ , while the CORALIE data result in the value of  $-5.3$  km s $^{-1}$  for the  $\gamma$ -velocity. Though the difference is small, homogeneity of the data and the identical treatment is a guarantee that the shift is not an artefact of the analysis. The individual data are listed in Tables 3 and 4.

SB of GH Car has to be verified by further observations.

**Table 3.** New RV values of GH Carinae from the SSO spectra. This is only a portion of the full version available online only.

JD <sub>⊙</sub> 240 0000+	<i>v</i> <sub>rad</sub> (km s <sup>-1</sup> )
533 64.2431	-8.4
533 67.2163	6.9
533 68.2542	-9.1
533 69.2434	-16.6
534 51.0951	-3.4

**Table 4.** New CORALIE velocities of GH Carinae. This is only a portion of the full version available online only.

JD <sub>⊙</sub> 240 0000+	<i>v</i> <sub>rad</sub> (km s <sup>-1</sup> )
556 52.8343	-9.9
556 53.8063	-13.7
556 54.6963	-8.9
556 55.6685	-2.0
556 56.6753	2.4

### 3.2 V419 Centauri

*Accurate value of the pulsation period.* The brightness variability of V419 Cen (HD 100148, *V* = 8.19 mag) was revealed by O’Leary & O’Connell (1937). This Cepheid also pulsates in the first overtone mode, so the *O* – *C* diagram was also constructed for the moments of the median brightness on the ascending branch, similar to the case of GH Car (see Section 3.1).

The *O* – *C* diagram of V419 Cen based on the *O* – *C* values listed in Table 5 is shown in Fig. 3. The plot can be approximated by a constant period by the ephemeris for the moments of median brightness on the ascending branch:

$$C = 2452\,357.3949 + 5.507\,123 \times E \pm 0.0053 \pm 0.000\,005. \quad (2)$$

However, a parabolic pattern indicating a continuously increasing period cannot be excluded. For the proper phasing of the RV data it is important that the *O* – *C* differences are about zero for each epoch when RV data were obtained.

*Binarity of V419 Cen.* All RV data (including the new ones listed in Table 6) have been folded on the accurate pulsation period taken from the ephemeris given in equation (2), so the different data series have been correctly phased with respect to each other. The merged RV phase curve is plotted in Fig. 4. The individual data series are denoted with different symbols: filled squares – RVs from 1952 by Stibbs (1955); empty triangles – data by Lloyd Evans (1980) from 1969 to 1970; filled and empty circles – our 2004–2005 and 2006 data, respectively.

Variability in the *γ*-velocity is striking. Systematic errors can be excluded. Although our 2006 data are shifted to a larger value of the *γ*-velocity, similarly to the case of GH Car (see Section 3.1), other new spectroscopic binaries and dozens of Cepheids in our sample with non-varying *γ*-velocities indicate stability of the equipment and reliability of the data reduction. Another piece of evidence in favour of the intrinsic variability of the *γ*-velocity is that both Stibbs

**Table 5.** *O* – *C* values of V419 Centauri (see the description in Section 3.1).

JD <sub>⊙</sub> 240 0000+	<i>E</i>	<i>O</i> – <i>C</i>	<i>W</i>	Data source
348 17.2512	-3185	+0.0431	2	Walraven et al. (1958)
352 19.2722	-3112	+0.0441	3	Irwin (1961)
402 85.8001	-2192	+0.0188	3	Stobie (1970)
407 37.4108	-2110	+0.0454	3	Pel (1976)
428 96.1636	-1718	+0.0060	3	Dean (1977)
443 00.3547	-1463	-0.1193	2	Berdnikov (2008)
446 30.7521	-1403	-0.1492	2	Eggen (1985)
481 66.4174	-761	-0.0569	3	<i>Hipparcos</i> (ESA 1997)
486 89.5720	-666	-0.0790	3	<i>Hipparcos</i> (ESA 1997)
495 43.1967	-511	-0.0583	2	Berdnikov (2008)
498 13.0946	-462	-0.0095	3	Berdnikov (2008)
503 85.8636	-358	+0.0187	2	Berdnikov (2008)
505 73.1155	-324	+0.0285	3	Berdnikov (2008)
509 03.5445	-264	+0.0301	3	Berdnikov (2008)
512 61.4846	-199	+0.0072	3	Berdnikov (2008)
516 47.0071	-129	+0.0311	3	Berdnikov (2008)
519 55.3943	-73	+0.0194	3	ASAS (Pojmanski 2002)
519 60.9164	-72	+0.0344	3	Berdnikov (2008)
521 26.0927	-42	+0.0030	3	ASAS (Pojmanski 2002)
523 57.3861	0	-0.0088	3	Berdnikov (2008)
524 67.5557	20	+0.0183	3	ASAS (Pojmanski 2002)
526 43.7458	52	-0.0195	3	Berdnikov (2008)
527 31.8585	68	-0.0208	3	ASAS (Pojmanski 2002)
530 12.7265	119	-0.0160	3	Berdnikov (2008)
530 62.2908	128	-0.0158	3	ASAS (Pojmanski 2002)
534 75.3737	203	+0.0328	3	ASAS (Pojmanski 2002)
535 24.8954	212	-0.0096	2	<i>INTEGRAL</i> OMC
537 89.2626	260	+0.0157	3	ASAS (Pojmanski 2002)
541 36.1005	323	-0.0951	1	<i>INTEGRAL</i> OMC
541 91.2873	333	+0.0204	3	ASAS (Pojmanski 2002)
545 87.8324	405	+0.0527	3	ASAS (Pojmanski 2002)
549 18.2426	465	+0.0355	3	ASAS (Pojmanski 2002)

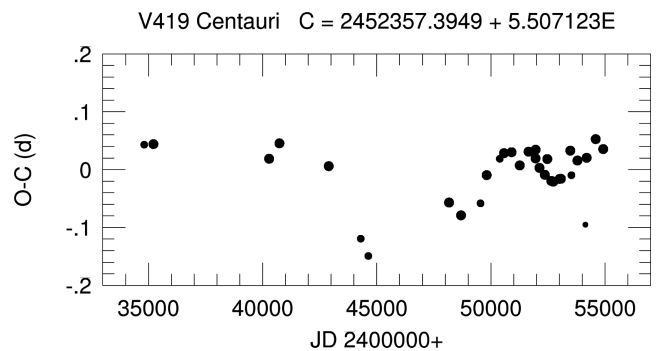


**Figure 3.** *O* – *C* diagram of V419 Cen. The plot can be approximated by a constant period but a parabolic pattern indicating a continuously increasing period cannot be excluded.

(1955) and Lloyd Evans (1980) used the same spectrograph during their observations.

To have a clearer picture, the *γ*-velocities (together with their uncertainties) are listed in Table 7 and also plotted in Fig. 5. The last two points (which are the most accurate ones), i.e. the shift between 2004–2005 and 2006 data implies an orbital period of several years instead of several decades suggested by the whole pattern of the plot.

**Table 6.** New RV values of V419 Centauri from the SSO spectra. This is only a portion of the full version available online only.

JD <sub>☉</sub> 240 0000+	<i>v</i> <sub>rad</sub> (km s <sup>-1</sup> )
533 69.2636	-1.8
534 51.1179	-4.8
534 52.0995	3.9
534 53.1895	-1.5
534 54.1215	-7.9

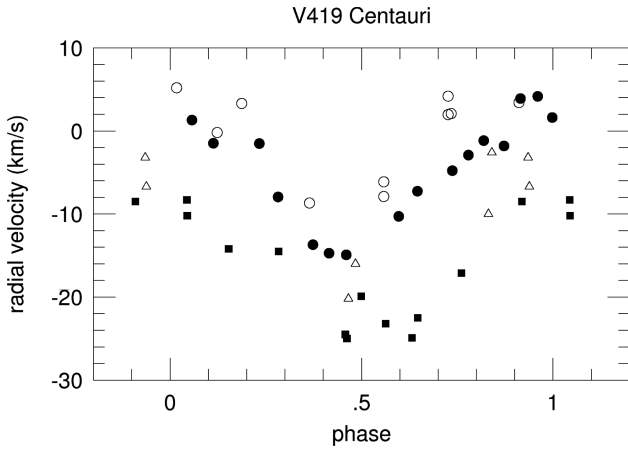


**Figure 4.** Merged RV phase curve of V419 Cen. There is a striking difference between the  $\gamma$ -velocities valid for the epoch of Stibbs' (1955) and Lloyd Evans' (1980) data (denoted as filled squares and empty triangles, respectively) and our recent data (denoted by circles, see the text).

**Table 7.**  $\gamma$ -velocities of V419 Centauri.

Mid-JD 240 0000+	<i>v</i> <sub><math>\gamma</math></sub> (km s <sup>-1</sup> )	$\sigma$ (km s <sup>-1</sup> )	Data source
341 29	-16.40	1.3	Stibbs (1955)
405 50	-11.70	1.5	Lloyd Evans (1980)
534 74	-5.53	0.3	This paper
538 00	-0.96	0.5	This paper

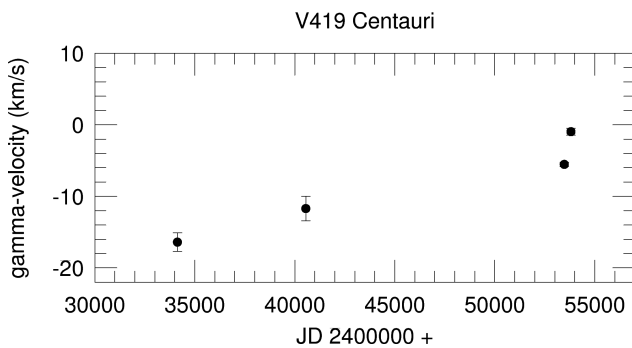


**Figure 5.** Temporal shift in the  $\gamma$ -velocity of V419 Cen.

### 3.3 V898 Centauri

*Accurate value of the pulsation period.* The brightness variability of V898 Cen (HD 97317,  $\langle V \rangle = 8.00$  mag) was revealed

**Table 8.**  $O - C$  values of V898 Centauri (description of the columns is given in Section 3.1).

JD <sub>☉</sub> 240 0000+	<i>E</i>	$O - C$	<i>W</i>	Data source
479 55.2823	-1247	+0.0023	3	<i>Hipparcos</i> (ESA 1997)
483 11.5410	-1146	+0.0027	3	<i>Hipparcos</i> (ESA 1997)
486 92.4782	-1038	-0.0096	3	<i>Hipparcos</i> (ESA 1997)
512 60.3772	-310	+0.0077	3	Berdnikov (2008)
516 48.3705	-200	-0.0031	3	Berdnikov (2008)
519 58.7588	-112	-0.0181	3	Berdnikov (2008)
523 53.8561	0	+0.0205	3	Berdnikov (2008)
526 50.1280	84	-0.0016	3	Berdnikov (2008)
530 06.4034	185	+0.0155	3	Berdnikov (2008)
531 40.4565	223	+0.0308	2	<i>INTEGRAL</i> OMC
537 18.7991	387	-0.1055	1	<i>INTEGRAL</i> OMC

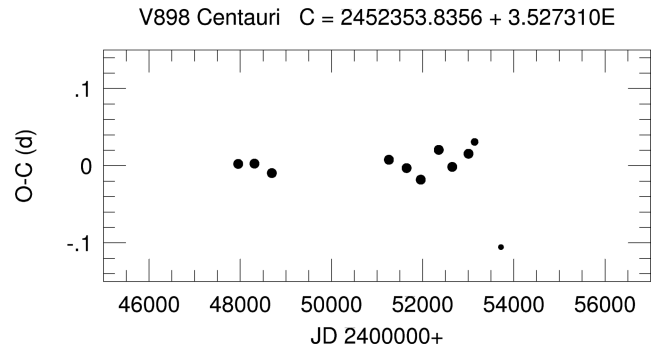


**Figure 6.**  $O - C$  diagram of V898 Cen. The plot can be approximated by a constant period.

by Strohmeier, Knigge & Ott (1964). This is also a low amplitude Cepheid pulsating in the first overtone mode. The first reliable photometric data were only obtained during the *Hipparcos* space astrometry mission (ESA 1997). Later on Berdnikov and his coworkers followed the photometric behaviour of V898 Cen (Berdnikov 2008).

The  $O - C$  diagram of V898 Cen was constructed for the moments of median brightness on the ascending branch (see Table 8). The weighted least-squares fit to the  $O - C$  values resulted in the ephemeris:

$$C = 2\,452\,353.8356 + 3.527\,310 \times E \pm 0.0052 \pm 0.000\,008. \quad (3)$$

The  $O - C$  diagram of V898 Cen plotted in Fig. 6 indicates constancy of the pulsation period.

*Binarity of V898 Cen.* The Cepheid variable V898 Cen has been neglected from the point of view of spectroscopy, as well. A spectral type of F3III has been assigned to it in the SIMBAD data base which is atypical of a Cepheid (and probably erroneous). Cepheids are supergiants of Iab or Ib luminosity class and their short period representatives have a late F spectral type. Ironically, there is a single RV data,  $-2.4 \pm 2.4$  km s<sup>-1</sup> (which is an average of two measurements) published by Nordström et al. (2004) in their catalogue of 14000 *dwarf* stars of F and G spectral types. However, the epoch of these particular observations has remained unknown. Therefore, our data provide a first epoch RV phase curve.

It became obvious already in the first observing season that an orbital effect is superimposed on the RV variations of pulsational origin (see the left-part of Fig. 7). Therefore, several spectra of V898

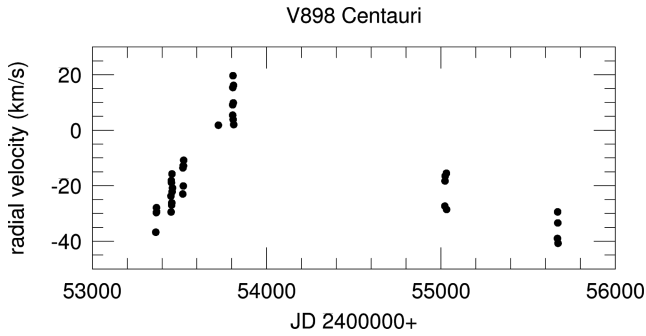


Figure 7. Merged RV curve of V898 Cen.

Table 9. New RV values of V898 Centauri from the SSO spectra. This is only a portion of the full version available online only.

JD <sub>⊙</sub> 240 0000+	$v_{\text{rad}}$ (km s <sup>-1</sup> )
533 64.2485	-36.8
533 67.2225	-29.7
533 68.2618	-27.9
533 69.2529	-29.4
534 51.1003	-23.7

Table 10. New FEROS velocities of V898 Centauri.

JD <sub>⊙</sub> 240 0000+	$v_{\text{rad}}$ (km s <sup>-1</sup> )
556 67.5948	-39.02
556 68.6044	-29.44
556 69.5644	-33.40
556 70.7789	-40.74

Cen have been taken in 2009 and 2011, as well. Our individual RV data are listed in Tables 9 and 10. Based on these data, the RV phase curve has been constructed using the 3.527 310 d pulsation period appearing in equation (3). The wide scatter in this phase curve plotted in Fig. 8 corresponds to a variable  $\gamma$ -velocity. The data series has been split into seven segments, denoted by different symbols in Fig. 8: empty circles – 2004 December; filled circles –

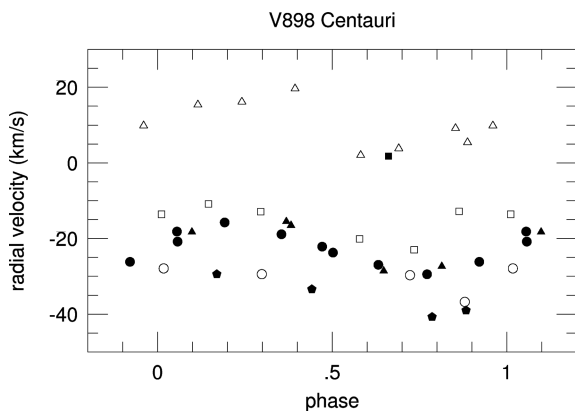


Figure 8. RV phase curve of V898 Cen. Various symbols refer to different observational runs (see the text).

Table 11.  $\gamma$ -velocities of V898 Centauri.

Mid-JD 240 0000+	$v_{\gamma}$ (km s <sup>-1</sup> )	$\sigma$ (km s <sup>-1</sup> )	Data source
533 67.7	-29.9	0.5	This paper
534 55.5	-22.8	0.4	This paper
535 21.4	-15.6	0.5	This paper
537 23.3	1.8	0.6	This paper
538 07.5	10.7	0.4	This paper
550 26.3	-21.8	0.5	This paper
556 69.2	-35.1	0.5	This paper

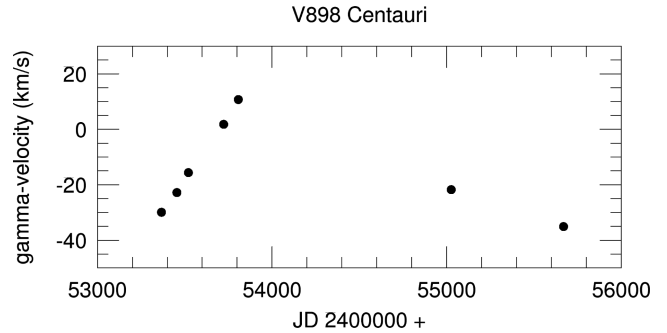


Figure 9. Temporal drift in the  $\gamma$ -velocity of V898 Centauri.

2005 March; empty squares – 2005 May–June; filled square – 2005 December; empty triangles – 2006 March; filled triangles – 2009 July and filled pentagons – 2011 April.

The  $\gamma$ -velocities determined from each data segment are listed in Table 11 and are plotted in Fig. 9. This latter plot implies that V898 Cen is a new spectroscopic binary and the orbital period is about 2000 or 3000 d, depending on whether the most negative value of the  $\gamma$ -velocity occurred before or after our measurements in 2011. The pattern of the points implies a non-sinusoidal shape of the orbital velocity phase curve, with much steeper ascending branch than descending one. This is a strong indication of an eccentric orbit; however, far more seasons of observations are needed before attempting to derive accurate orbital elements from the  $\gamma$ -velocity variations. The most important feature of Fig. 9 is the large amplitude of the orbital velocity variations: it exceeds 40 km s<sup>-1</sup>. The ‘recorder’ among the known binary systems involving a Cepheid component has been the system of SU Cygni with a peak-to-peak orbital amplitude of 60 km s<sup>-1</sup> (see the online data base of Cepheids in binary systems described by Szabados 2003a).

The orbital motion of the Cepheid component around the centre of mass in the binary system may cause a light-time effect in the  $O - C$  diagram of the given variable star. In the case of V898 Cen the wave-like pattern characteristic of the light-time effect cannot be detected yet (see Fig. 6).

To provide reliable values for the physical properties of this bright Cepheid, our FEROS spectra were analysed in detail. The parameters  $T_{\text{eff}}$ ,  $\log g$ ,  $[M/H]$  and  $v \sin i$  were determined by searching for the best-fitting model in the synthetic spectrum library of Munari et al. (2005) using a standard  $\chi^2$  procedure. To derive the parameters and their errors we applied the following method. The model spectra were ordered according to their calculated  $\chi^2$  value, then we selected all with number less than  $1.05 \chi^2_{\text{min}}$  and adopted the means and the standard deviations of this sample as values and errors of the parameters.

The best-fitting values are as follows:

$$T_{\text{eff}} = 5950 \pm 380 \text{ K},$$

$$\log g = 1.2 \pm 0.7,$$

$$[M/H] = -0.4 \pm 0.2$$

$$v \sin i = 2 \pm 2.$$

The effective temperature obtained by us corresponds to an F9 spectral type supergiant star, a typical value of a short-period Cepheid. Note, however, that these values are preliminary ones. The large number of SSO spectra of all 40 target Cepheids will be analysed for obtaining physical properties with smaller uncertainties.

### 3.4 AD Puppis

*Accurate value of the pulsation period.* The brightness variability of AD Pup (HD 63446,  $V = 9.91$  mag) was revealed by Hertzprung (Wesselink 1935). This is the longest period Cepheid in this paper and it has been frequently observed from the 1950s. Long-period Cepheids are usually fundamental pulsators and they oscillate with a large amplitude. In their case, the  $O - C$  analysis is based on the moments of brightness maxima.

The  $O - C$  differences of AD Puppis are listed in Table 12. These values have been obtained by the following ephemeris:

$$C = 2451935.3031 + 13.596919 \times E \pm 0.0065 \pm 0.000040 \quad (4)$$

**Table 12.**  $O - C$  values of AD Puppis (description of the columns is given in Section 3.1 but the first column contains the moments of brightness maxima).

$JD_{\odot}$ 240 0000+	$E$	$O - C$	$W$	Data source
346 14.2663	-1274	+1.4380	1	Walraven et al. (1958)
352 12.4702	-1230	+1.3775	2	Irwin (1961)
408 81.6304	-813	+0.6224	3	Pel (1976)
416 56.4884	-756	+0.4561	3	Madore (1975)
445 52.3367	-543	+0.1606	2	Eggen (1983)
456 94.4366	-459	+0.1193	2	Berdnikov (2008)
479 24.3692	-295	+0.1572	2	<i>Hipparcos</i> (ESA 1997)
484 00.1048	-260	+0.0006	3	<i>Hipparcos</i> (ESA 1997)
487 67.2244	-233	+0.0034	2	<i>Hipparcos</i> (ESA 1997)
498 14.2750	-156	+0.0913	3	Berdnikov (2008)
508 06.7186	-83	-0.0402	2	Berdnikov (2008)
512 69.0641	-49	+0.0100	3	Berdnikov (2008)
516 49.8321	-21	+0.0643	3	Berdnikov (2008)
519 35.3197	0	+0.0166	3	ASAS (Pojmanski 2002)
519 62.5484	2	+0.0515	3	Berdnikov (2008)
522 34.5236	22	+0.0883	3	ASAS (Pojmanski 2002)
523 43.2076	30	-0.0031	3	Berdnikov (2008)
524 11.1912	35	-0.0041	3	ASAS (Pojmanski 2002)
526 42.3572	52	+0.0143	3	Berdnikov (2008)
527 23.9484	58	+0.0240	3	ASAS (Pojmanski 2002)
529 95.8827	78	+0.0199	3	Berdnikov (2008)
530 50.3131	82	+0.0626	3	ASAS (Pojmanski 2002)
532 54.2231	97	+0.0189	3	<i>INTEGRAL</i> OMC
534 44.5663	111	+0.0052	3	ASAS (Pojmanski 2002)
537 70.8223	135	-0.0649	3	ASAS (Pojmanski 2002)
538 52.4136	141	-0.0551	3	ASAS (Pojmanski 2002)
541 78.8427	165	+0.0480	3	ASAS (Pojmanski 2002)
545 32.3418	191	+0.0272	3	ASAS (Pojmanski 2002)
548 31.3885	213	-0.0583	3	ASAS (Pojmanski 2002)

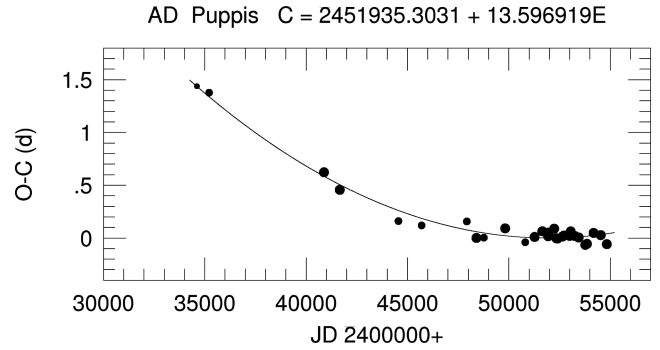


**Figure 10.**  $O - C$  diagram of AD Pup. The plot can be approximated by a parabola indicating a continuously increasing pulsation period.

which contains the constant and linear terms of the weighted parabolic fit to the  $O - C$  values. The parabolic nature of the  $O - C$  diagram is clearly seen in Fig. 10.

This parabolic trend corresponds to a continuous period increase of  $(1.7 \pm 0.09) \times 10^{-6}$  d cycle $^{-1}$ , i.e.  $\Delta P = 0.004567$  d century $^{-1}$ . This tiny but non-negligible period increase has been caused by stellar evolution: while the Cepheid crosses the instability region towards lower temperatures in the Hertzsprung–Russell diagram, its pulsation period is increasing. Continuous period variations (of either sign) often occur in the pulsation of long-period Cepheids (Szabados 1983).

The pattern of fluctuations around the fitted parabola shows a wavy nature with a characteristic period of about 50 years as if it were a light-time effect.

*Binarity of AD Pup.* The earlier RV data by Joy (1937) imply a significantly different  $\gamma$ -velocity ( $66.5$  km s $^{-1}$ ) than our recent ones ( $74.0$  km s $^{-1}$ ) in spite of the uncertainty of his individual data as large as  $4$  km s $^{-1}$ . Because the zero-point of Joy's system is reliable, as discussed by Szabados (1996), there is no systematic difference of instrumental or data treatment origin between Joy's and the more recent observational series. The only plausible explanation for the shift in the  $\gamma$ -velocity is the orbital motion in a binary system superimposed on the pulsational RV changes. The shift in the  $\gamma$ -velocity is obvious in the phase diagram of the RVs of AD Puppis plotted in Fig. 11 where Joy's data are denoted with empty squares, while our data are represented with filled circles. The  $\gamma$ -velocity of AD

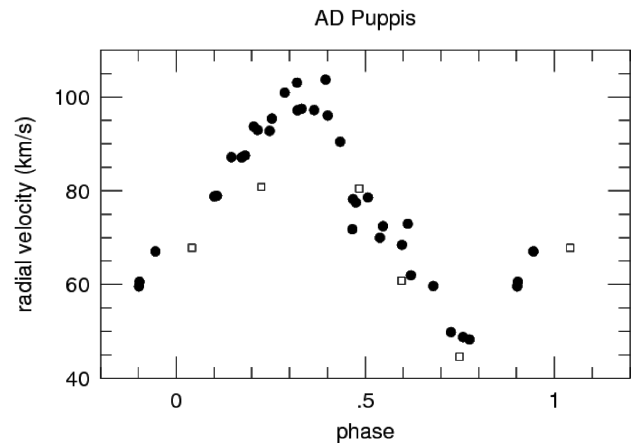


**Figure 11.** Merged RV phase curve of AD Pup. There is an obvious shift between the  $\gamma$ -velocities valid for the epoch of Joy's (1937) data (denoted by empty squares) and our data (filled circles).

**Table 13.** New RV values of AD Pup-pis from the SSO spectra. This is only a portion of the full version available online only.

JD <sub>⊙</sub> 2 400 000+	$v_{\text{rad}}$ (km s <sup>-1</sup> )
533 04.2658	103.1
533 06.2580	71.8
533 07.2487	70.0
533 08.2504	72.9
533 09.1650	59.7

Pup did not change notably during the interval of our observations. Our RV data (listed in Table 13) have been folded with the period as given in the ephemeris in equation (4). Joy's data have been phased with the same period but a proper correction has been applied to correct for the phase shift due to the parabolic  $O - C$  graph.

The smaller value of the  $\gamma$ -velocity determined from Joy's (1937) data is in a qualitative agreement with the wave-like pattern superimposed on the fitted parabola in Fig. 10. In this particular case, the light-time effect interpretation implies a 50 year-long orbital period.

### 3.5 AY Sagittarii

*Accurate value of the pulsation period.* The brightness variability of AY Sgr (HIP 90110,  $\langle V \rangle = 10.55$  mag) was revealed by Henrietta Leavitt (Pickering 1904). Hoffmeister (1923) determined the pulsation period to be 6.744 26 d from his unpublished visual observations made in 1917–1918. Interestingly enough, this period is about 3 per cent longer than the value deduced from the  $O - C$  diagram (see Table 14 and Fig. 12). Such a strong period change, if it really happened, is unprecedented among classical Cepheids.

**Table 14.**  $O - C$  values of AY Sagittarii (description of the columns is given in Section 3.1 but the first column contains the moments of brightness maxima).

JD <sub>⊙</sub> 2400000+	$E$	$O - C$	$W$	Data source
214 25.45	-4722	-2.04	-	Hoffmeister (1923)
270 51.2394	-3866	0.1098	1	Florya & Kukarkina (1953)
349 60.9601	-2662	-0.0485	3	Walraven et al. (1958)
368 13.6830	-2380	+0.0283	3	Weaver, Steinmetz & Mitchell (1960)
407 81.6694	-1776	-0.0642	3	Pel (1976)
439 08.8993	-1300	+0.0042	2	Harris (1980)
483 30.3254	-627	+0.0444	2	<i>Hipparcos</i> (ESA 1997)
499 46.4248	-381	+0.0057	2	Berdnikov (2008)
509 05.5915	-235	+0.0010	3	Berdnikov (2008)
512 73.5280	-179	+0.0027	3	Berdnikov (2008)
516 47.9618	-122	-0.0010	3	Berdnikov (2008)
520 88.1177	-55	-0.0128	3	ASAS (Pojmanski 2002)
524 49.4780	0	+0.0158	3	ASAS (Pojmanski 2002)
528 43.6666	60	+0.0244	3	ASAS (Pojmanski 2002)
529 09.3756	70	+0.0367	3	<i>INTEGRAL</i> OMC
530 93.2519	98	-0.0377	3	Berdnikov (2008)
531 65.5436	109	-0.0123	3	ASAS (Pojmanski 2002)
535 59.7519	169	+0.0160	3	ASAS (Pojmanski 2002)
538 61.9333	215	-0.0073	3	ASAS (Pojmanski 2002)
543 41.5068	288	-0.0195	3	ASAS (Pojmanski 2002)
546 50.3169	335	+0.0163	2	<i>INTEGRAL</i> OMC
547 42.2598	349	-0.0162	3	ASAS (Pojmanski 2002)
549 85.3351	386	-0.0186	3	ASAS (Pojmanski 2002)

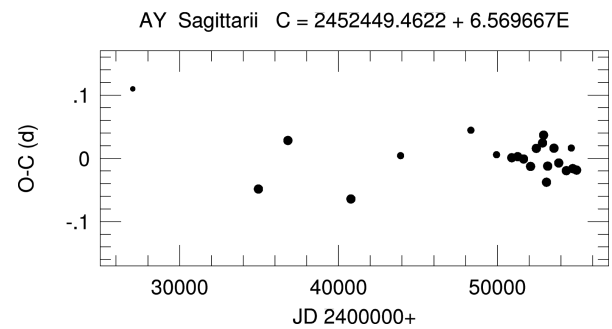


**Figure 12.**  $O - C$  diagram of AY Sgr. The plot can be approximated by a constant period.

**Table 15.** New RV values of AY Sagittarii from the SSO spectra. This is only a portion of the full version available online only.

JD <sub>⊙</sub> 240 0000+	$v_{\text{rad}}$ (km s <sup>-1</sup> )
534 51.2048	-12.9
534 52.2318	-6.1
534 53.2541	5.3
534 54.2702	-29.7
534 55.2032	-32.7

AY Sgr is a fundamental mode pulsator, so its  $O - C$  diagram has been constructed based on the moments of brightness maxima. The tabulated  $O - C$  values have been calculated by using the ephemeris:

$$C = 2\,452\,449.4622 + 6.569\,667 \times E \pm 0.0044 \pm 0.000\,004 \quad (5)$$

based on applying a weighted linear least-squares fit to the  $O - C$  differences.

As is seen in Fig. 12, the pulsation period of AY Sgr has remained practically constant over decades.

*Binarity of AY Sgr.* Our new RV data are listed in Table 15. The first epoch RV phase curve of AY Sgr by Joy (1937) has been followed by our one 25 000 d later. The merged RV phase curve in Fig. 13 shows a significant increase in the  $\gamma$ -velocity during eight decades: at JD 242 7640  $v_{\gamma} = -22.4$  km s<sup>-1</sup>, while at JD 245 3550  $v_{\gamma} = -15.5$  km s<sup>-1</sup> indicating the membership of AY Sgr in a spectroscopic binary system. During the two observing seasons covered by our spectroscopic observations, no shift in the  $\gamma$ -velocity is apparent. Nevertheless, the larger amplitude of the phase curve based on Joy's data may be the consequence of the orbital motion in the binary system during his five-year-long observational interval.

### 3.6 ST Velorum

*Accurate value of the pulsation period.* The brightness variability of ST Vel (CD -50° 3533),  $\langle V \rangle = 9.73$  mag) was suspected by Kapteyn (Gill & Innes 1903) and it was reported as a new variable by Cannon et al. (1909). Being a Cepheid that pulsates in the fundamental mode, the  $O - C$  diagram in Fig. 14 has been constructed for the moments of brightness maxima listed in Table 16. The final ephemeris obtained by a weighted parabolic least-squares fit is

$$C = 2\,451\,939.5962 + 5.858\,316 \times E \pm 0.0025 \pm 0.000\,006. \quad (6)$$

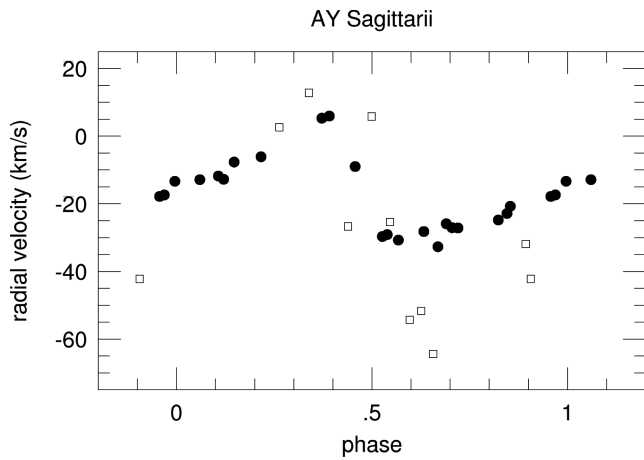


**Figure 13.** Merged RV phase curve of AY Sgr. There is a striking difference between the  $\gamma$ -velocities valid for the epoch of Joy's (1937) data (denoted as empty squares) and our recent data (filled circles).

The second-order term omitted from equation (6) results in a continuous increase in the pulsation period amounting to  $(3.04 \pm 0.58) \times 10^{-8} \text{ d cycle}^{-1}$ , i.e.  $16.36 \text{ s century}^{-1}$ .

*Binarity of ST Vel.* The available RV data – those by Pont et al. (1994) and our new ones listed in Table 17 – have been plotted in Fig. 15. When folding the data into a phase curve, the period of 5.858 316 d given in the equation (6) was used but due to the parabolic pattern of the  $O - C$  graph, a tiny correction was applied when plotting the data by Pont et al. (1994). It is noteworthy that our own data show an excessive scatter that can be explained in terms of the variation in the  $\gamma$ -velocity. This effect is clearly seen in Fig. 16 where the annual  $\gamma$ -velocities listed in Table 18 have been plotted. The pattern of the points in this figure implies that the orbital period can be several hundred days, which is rather short among the spectroscopic binaries containing a Cepheid component.

#### 4 CONCLUSIONS

We pointed out that six southern Galactic Cepheids, GH Carinae, V419 Centauri, V898 Centauri, AD Puppis, AY Sagittarii and ST Velorum have a variable  $\gamma$ -velocity which implies their membership in spectroscopic binary systems. The available RV data are insufficient to determine the orbital period and other elements of the orbit. We can only state that the orbital period of V419 Cen is several years, for V898 Cen it is 2000–3000 d, for AD Pup about 50 years, and for ST Vel several hundred days.

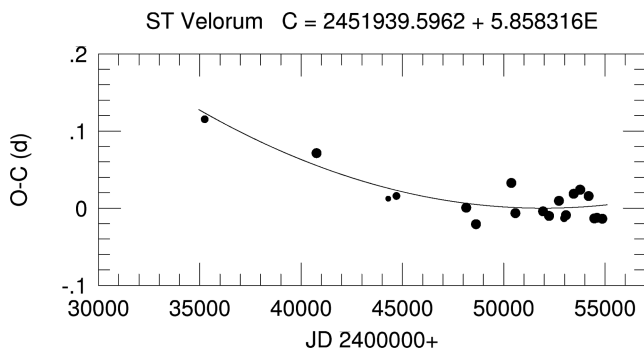


**Figure 14.**  $O - C$  diagram of ST Vel. The plot can be approximated by a parabola indicating a continuous period increase.

**Table 16.**  $O - C$  values of ST Velorum (description of the columns is given in Section 3.1 but the first column contains the moments of brightness maxima).

JD <sub>⊙</sub> 240 0000+	<i>E</i>	<i>O - C</i>	<i>W</i>	Data source
352 43.5109	-2850	+0.1153	2	Walraven et al. (1958)+ Irwin (1961)
407 62.0007	-1908	+0.0714	3	Pel (1976)
443 00.3645	-1304	+0.0124	1	Berdnikov (2008)
447 04.5918	-1235	+0.0159	2	Eggen (1985)
481 49.2664	-647	+0.0007	3	<i>Hipparcos</i> (ESA 1997)
486 29.6270	-565	-0.0207	3	<i>Hipparcos</i> (ESA 1997)
503 75.4585	-267	+0.0327	3	Berdnikov (2008)
505 74.6022	-233	-0.0064	3	Berdnikov (2008)
519 39.5921	0	-0.0041	3	ASAS (Pojmanski 2002)
522 38.3603	51	-0.0100	3	ASAS (Pojmanski 2002)
527 24.6201	134	+0.0096	3	ASAS (Pojmanski 2002)
529 76.5052	177	-0.0129	2	<i>INTEGRAL</i> OMC
530 70.2422	193	-0.0090	3	ASAS (Pojmanski 2002)
534 51.0604	258	+0.0187	3	ASAS (Pojmanski 2002)
537 67.4149	312	+0.0241	3	<i>INTEGRAL</i> OMC
537 79.1313	314	+0.0239	3	ASAS (Pojmanski 2002)
541 89.2053	384	+0.0158	3	ASAS (Pojmanski 2002)
544 70.3755	432	-0.0132	3	ASAS (Pojmanski 2002)
545 99.2593	454	-0.0124	3	ASAS (Pojmanski 2002)
548 62.8823	499	-0.0136	3	ASAS (Pojmanski 2002)

**Table 17.** New RV values of ST Velorum from the SSO spectra. This is only a portion of the full version available online only.

JD <sub>⊙</sub> 240 0000+	<i>v</i> <sub>rad</sub> (km s <sup>-1</sup> )
533 10.2539	-12.9
533 12.2108	-1.9
533 64.2096	-9.1
533 67.1854	18.5
534 50.9950	-6.8

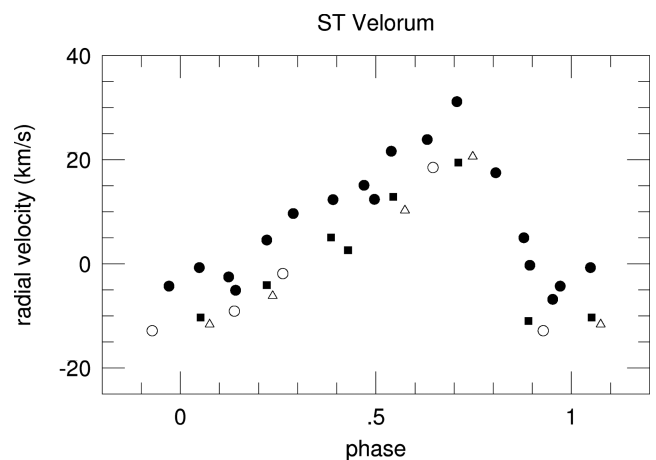


**Figure 15.** Merged RV phase curve of ST Vel. The triangles represent RVs obtained by Pont, Burki & Mayor (1994), our data are split into three parts: those from 2004 (empty circles), from 2005 (filled circles) and 2006 (filled squares).

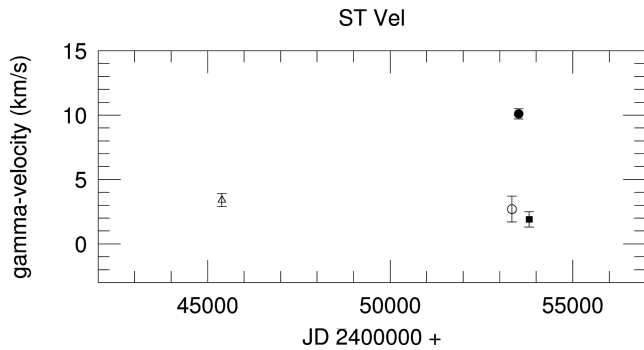


**Figure 16.** Temporal variations in the  $\gamma$ -velocity of ST Velorum. The symbols are consistent with those used in Fig. 15.

**Table 18.**  $\gamma$ -velocities of ST Velorum.

Mid-JD 2400000+	$v_\gamma$ (km s <sup>-1</sup> )	$\sigma$ (km s <sup>-1</sup> )	Data source
453 92	3.4	0.5	Pont et al. (1994)
533 35	2.7	1.0	This paper
535 20	10.1	0.4	This paper
538 08	1.9	0.6	This paper

The value of the orbital period for spectroscopic binary systems involving a Cepheid component is often unknown: according to the online data base (Szabados 2003a) the orbital period has been determined for about 20 per cent of the known SB Cepheids. Majority of the known orbital periods exceeds a thousand days.

Our finding confirms the previous statement by Szabados (2003a) about the high percentage of binaries among classical Cepheids and the observational selection effect hindering the discovery of new cases.

RV data obtained prior to ours were instrumental in discovering binarity of V419 Cen, AD Pup, AY Sgr and ST Vel, while the spectroscopic binary nature of GH Car and V898 Cen has been discovered from our observations alone.

A companion star may have various effects on the photometric properties of the Cepheid component. Various pieces of evidence of duplicity based on the photometric criteria are discussed by Szabados (2003b) and Klagyivik & Szabados (2009). As to our targets, there is no obvious sign of companion from photometry alone. This indicates that the companion star cannot be much hotter than the Cepheid component in either case. Nevertheless, weak evidence of anomalous photometric behaviour was reported for GH Car by Madore & Fernie (1980) (abnormal phase shift between the light curves in different photometric bands) and for V419 Cen by Onembo et al. (1985) (anomalous behaviour when determining its physical parameters with the CORS method). The strange spectral type of F3III for V898 Cen appearing in the SIMBAD data base may be wrong because an F9 spectral type has been deduced from our spectra. Further spectroscopic observations are necessary to characterize these binary systems. In addition, accurate future photometric observations can be instrumental in confirming the interpretation of the wavy pattern superimposed on the parabolic  $O - C$  graph of AD Pup in terms of a light-time effect.

Regular monitoring of the RVs of a large number of Cepheids will be instrumental in finding more long-period spectroscopic binaries among Cepheids. Quite recently, Evans et al. (2012) reported on their on-going survey for pointing out binarity of Cepheids from the existing RV data covering sufficiently long time interval. RV data to

be obtained with the *Gaia* astrometric space probe (expected launch: October 2013) will certainly result in revealing new spectroscopic binaries among Cepheids brighter than 13 and 14 mag (Eyer et al. 2012).

When determining the physical properties (luminosity, temperature, radius, etc.) of individual Cepheids, the effects of the companion on the observed parameters (apparent brightness, colour indices, etc.) have to be corrected for. This type of analysis, however, should be preceded by revealing the binarity of the given Cepheid.

## ACKNOWLEDGEMENTS

This project has been supported by the ESA PECS Project C98090, ESTEC Contract No. 4000106398/12/NL/KML, the Hungarian OTKA Grants K76816, K83790, K104607 and MB08C 81013, as well as the European Community's Seventh Framework Programme (FP7/2007-2013) under grant agreement no. 269194 and the 'Lendület-2009' Young Researchers Programme of the Hungarian Academy of Sciences. AD was supported by the Hungarian Eötvös fellowship. AD has been supported by the János Bolyai Research Scholarship of the Hungarian Academy of Sciences. AD is very thankful to the staff at The Lodge in Siding Spring Observatory for their hospitality and the very nice food, making the time spent there lovely and special. Part of the research leading to these results has received funding from the European Research Council under the European Community's Seventh Framework Programme (FP7/2007-2013)/ERC grant agreement no. 227224 (PROSPERITY). The *INTEGRAL* photometric data, pre-processed by ISDC, have been retrieved from the OMC Archive at CAB (INTA-CSIC). Critical remarks by Dr. Mária Kun and the referee's suggestions led to a considerable improvement in the presentation of the results.

## REFERENCES

- Baranne A. et al., 1996, *A&AS*, 119, 373  
 Berdnikov L. N., 2008, *VizieR On-line Data Catalog: II/285*  
 Cannon A., Wells L. D., Leland E. F., Pickering E. C., 1909, *Harvard Coll. Obs. Circ.*, 15, 1  
 Dean J. F., 1977, *Mon. Not. Astron. Soc. South. Afr.*, 36, 3  
 Derekas A. et al., 2012, *MNRAS*, 425, 1312  
 Eggen O. J., 1983, *AJ*, 88, 998  
 Eggen O. J., 1985, *AJ*, 90, 1297  
 ESA, 1997, *The Hipparcos and Tycho Catalogues*, ESA SP-1200. ESA, Noordwijk  
 Evans N. R. et al., 2012, *AAS Meeting*, 220, 329.07  
 Eyer L. et al., 2012, *Ap&SS*, 341, 207  
 Florya N. F., Kukarkina N. P., 1953, *Sternberg Trudy*, 23, 5  
 Gill D., Innes R. T. A., 1903, *Cape Ann.*, 9, 9B  
 Harris H. C., 1980, PhD thesis, Washington University, Seattle  
 Hertzsprung E., 1930, *Bull. Astron. Inst. Neth.*, 6, 6  
 Hoffmeister C., 1923, *Astron. Nachr.*, 218, 325  
 Irwin J. B., 1961, *ApJS*, 6, 253  
 Joy A. H., 1937, *ApJ*, 86, 363  
 Kaufer A., Stahl O., Tubbesing S., Nørregaard P., Avila G., Francois P., Pasquini L., Pizzella A., 1999, *Messenger*, 95, 8  
 Kaufer A., Stahl O., Tubbesing S., Nørregaard P., Avila G., Francois P., Pasquini L., Pizzella A., 2000, in Iye M., Moorwood A. F., eds, *Proc. SPIE Ser. Vol. 4008, Optical and IR Telescope Instrumentation and Detectors*. SPIE, Bellingham, p. 459  
 Klagyivik P., Szabados L., 2009, *A&A*, 504, 959  
 Lloyd Evans T., 1980, *South Afr. Astron. Obser. Circ.*, 1, 257  
 Madore B. F., 1975, *ApJS*, 29, 219  
 Madore B. F., Fernie J. D., 1980, *PASP*, 92, 315  
 Munari U., Sordo R., Castelli F., Zwitter T., 2005, *A&A*, 442, 1127

- Nordström B. et al., 2004, *A&A*, 418, 989  
 O'Leary W., O'Connell D., 1937, *Astron. Nachr.*, 264, 141  
 Onnembo A., Buonaura B., Caccin B., Russo G., Sollazzo C., 1985, *A&A*, 152, 349  
 Pel J. W., 1976, *A&AS*, 24, 413  
 Pepe F., Mayor M., Galland F., Naef D., Queloz D., Santos N. C., Udry S., Burnet M., 2002, *A&A*, 388, 632  
 Pickering E. C., 1904, *Harvard Coll. Obs. Circ.*, 91, 1  
 Pojmanski G., 2002, *Acta Astron.*, 52, 397  
 Pont F., Burki G., Mayor M., 1994, *A&AS*, 105, 165  
 Queloz D. et al., 2001, *Messenger*, 105, 1  
 Sterken C., 2005, in Sterken C., ed., *ASP Conf. Ser. Vol. 335, The Light-Time Effect in Astrophysics*. Astron. Soc. Pac., San Francisco, p. 3  
 Stibbs D. W. N., 1955, *MNRAS*, 115, 363  
 Stobie R. S., 1970, *MNRAS*, 148, 1  
 Strohmeier W., Knigge R., Ott H., 1964, *Inf. Bull. Var. Stars*, 66, 1  
 Szabados L., 1983, *Ap&SS*, 96, 185  
 Szabados L., 1996, *A&A*, 311, 189  
 Szabados L., 2003a, *Inf. Bull. Var. Stars*, 5394, 1  
 Szabados L., 2003b, *Recent Res. Dev. Astron. & Astrophys.*, 1, 787  
 Szabados L., Klagyivik P., 2012, *Ap&SS*, 341, 99  
 Walraven Th., Muller A. B., Oosterhoff P. T., 1958, *Bull. Astron. Inst. Neth.*, 14, 81  
 Weaver H. F., Steinmetz D., Mitchell R., 1960, *Lowell Obser. Bull.*, 5, 30  
 Wesselink A. J., 1935, *Bull. Astron. Inst. Neth.*, 7, 243  
 Wilson D. M. et al., 2008, *ApJ*, 675, L113

## SUPPORTING INFORMATION

Additional Supporting Information may be found in the online version of this article:

**Table 3.** New RV values of GH Carinae from the SSO spectra.

**Table 4.** New CORALIE velocities of GH Carinae.

**Table 6.** New RV values of V419 Centauri from the SSO spectra.

**Table 9.** New RV values of V898 Centauri from the SSO spectra.

**Table 13.** New RV values of AD Puppis from the SSO spectra.

**Table 15.** New RV values of AY Sagittarii from the SSO spectra.

**Table 17.** New RV values of ST Velorum from the SSO spectra. (<http://www.mnras.oxfordjournals.org/lookup/suppl/doi:10.1093/mnras/stt027/-/DC1>).

Please note: Oxford University Press are not responsible for the content or functionality of any supporting materials supplied by the authors. Any queries (other than missing material) should be directed to the corresponding author for the article.

This paper has been typeset from a  $\text{T}_{\text{E}}\text{X}/\text{L}^{\text{A}}\text{T}_{\text{E}}\text{X}$  file prepared by the author.